G-Theory → Maxwell Duality: Lie-N Compactification, a Nonsingular Bounce, and Topological Photon Signatures

: Prospects for evidence of an unobserved extended Maxwell law

P. De Ceuster*

September 28, 2025

Abstract

As the photon travels, we can anticipate the surroundings of the photon. In this work, we present further evidence related to an unobserved law of nature by working with our Maxwell extensions. We will deliberate cause a reformulation of a Lie-N G-theory cosmogenesis program we will define foremost. Starting from algebraic G0/Gp actions built on Lie-N brackets, we perform a consistent dimensional reduction and show how structurally-determined higher-curvature and form-coupling terms produce an event that involves, always a nonsingular cosmological bounce. Because the bounce always seems to take place, concurrently, a pushforward of a Higgs/C-field morphism yields a conserved topological 3-form current J_s, which minimally modifies Maxwell's equations to

$$\mathrm{d}\big(*F - J_s\big) = 0.$$

Since our extension seems to manifest, we hence prove a Soul-Charge Duality theorem , part of which we have established in earlier works. Hence we are, through this new abstract establishing a map between microscopic compactification data and the triplet (α, β, ω) controlling the gravitational bounce and the electromagnetic topological imprint, respectively. The duality hence links bounce-resolving microphysics and tiny photon-phase effects, opening both cosmological and laboratory windows (interferometry, polarization) to test a previously unobserved extension of Maxwell's law. In order to further provide sufficient depth into our investigation we will derive the effective 4D action, present analytic and numerical bounce solutions free of obvious ghost instabilities, compute linear perturbations, discuss anomaly consistency, and forecast experimental bounds.

*Dedicated to Bronisława Dłuska - the sister of Marie

Contents

1 Introduction to an unobserved law of nature

Big scientific problems require big solutions. The initial singularity problem remains central in theoretical cosmology yet many questions arise. Approaches include loop quantum cosmology, higher-derivative gravity, and string/brane-inspired models but these fall short in relation to our need to achieve a deeper understanding in the field of photonics. In one of the more recent works published around G-theory, (see [2]) wormhole/BIon constructions were deployed to produce oscillatory cosmologies. We take note of G-theory, however in order to study photonic laws, here we construct a proper algebraic backbone (Lie-N brackets, G0/Gp actions, brane creation from “nothing”) but we do not cover any wormholes or dependence on wormholes; we stick to classical physics and classical mechanism instead and we derive a bounce from effective higher-curvature or effective-stress terms that appear after dimensional reduction. This allows us to track our photon travelling through higher dimensions properly.

Simultaneously, as we track our photon travelling through higher dimensions, we incorporate a second, dual angle: via a pushforward of internal Higgs/C-field data we obtain a topological 3-form J_s on spacetime, which minimally modifies Maxwell’s equations in the 4D effective theory. The central claim is *soul-charge duality*: the same compactification data determine both the curvature coefficients that allow a bounce and the cohomology class controlling J_s, so cosmological singularity resolution and tiny photon effects share a common origin and become jointly testable. The bounce is always there, and an unobserved law becomes observable.

2 The impossible turns possible: Lie-N algebra and G-theory foundations

We recall the central algebraic building blocks crucial to our stance. The Lie-N bracket is an alternating multilinear map

$$[X_1, \ldots, X_N]_N = f_{\alpha_1 \cdots \alpha_N}{}^{\alpha}\, X^{\alpha_1} \otimes \cdots \otimes X^{\alpha_N},$$

with generalized Jacobi identities constraining the structure constants f. A prototypical scalar-sector G0 action is written schematically as

$$S_{G0} = T_{G0} \int \mathrm{d}t \ \mathrm{Tr} \Big\langle [X_{L_1}, \ldots, X_{L_N}]_N \, , [X_{L_1}, \ldots, X_{L_N}]_N \Big\rangle, \qquad (1)$$

where T_{G0} is a tension-like normalization and the trace pairs algebraic indices.

Higher-rank excitations (forms, vectors) arise naturally as modes of the algebraic variables; compactifications and consistent truncations of Gp actions will produce the effective 4D fields we study. For notational clarity we relegate long definitions and the original Sepehri–Pincak expressions to Appendix A. First things first: reduction.

3 Dimensional reduction and the effective 4D action

We will adopt a product ansatz for the higher-dimensional manifold that suits our needs:

$$\mathcal{Y} = X_4 \times K_{M-4},$$

with coordinates x^μ on X_4 and y^a on K. We perform a harmonic-type expansion of the algebraic fields and integrate over K, consistently truncating to light modes relevant for cosmology and photon dynamics. As light moves, we can study the surroundings involved. It is important to note ,to leading nontrivial order the resulting effective action on X_4 has the schematic form

$$S_{\text{eff}} = \int_{X_4} \mathrm{d}^4x\sqrt{-g}\Big[\tfrac{M_{\text{Pl}}^2}{2}R + \alpha R^2 + \beta R_{\mu\nu}R^{\mu\nu} - \tfrac{1}{4}F_{\mu\nu}F^{\mu\nu} + \mathcal{L}_{\text{matter}}^{\text{eff}}\Big] + q_s\int_{X_4} A\wedge J_s. \tag{2}$$

where the coefficients α, β are calculable integrals over K involving structure constants, internal curvature, and compactification radii. The S_{J_s} term (introduced in Sec. 5) encodes couplings that push forward to the 3-form J_s.

Long algebraic manipulations appear in Appendix A; here we focus on the physical consequences. This is a first realization: the physical consequences are next. Varying the effective action (2) with respect to the gauge potential A gives the modified Maxwell equation

$$\mathrm{d}(*F) \;=\; q_s J_s. \tag{3}$$

Gauge invariance under $A \mapsto A + \mathrm{d}\lambda$ shifts the action by $q_s \int_{X_4} \mathrm{d}\lambda \wedge J_s = -q_s \int_{X_4} \lambda\, \mathrm{d}J_s$, so consistency requires $\mathrm{d}J_s = 0$ (ensured by the pushforward of a closed internal form; see Appendix B).

Gauge invariance under $A \to A + \mathrm{d}\lambda$ shifts the action by $q_s \int \mathrm{d}\lambda \wedge J_s = -q_s \int \lambda\, \mathrm{d}J_s$, which vanishes precisely when $\mathrm{d}J_s = 0$. Thus consistency requires J_s to be closed, as guaranteed by its construction as a pushforward of an internal closed form.

For clarity we rewrite the higher-curvature sector in Planck-normalized form

$$S_{\text{grav}} = \frac{M_{\text{Pl}}^2}{2}\int \mathrm{d}^4x\sqrt{-g}\Big[R + \alpha' R^2 + \beta' R_{\mu\nu}R^{\mu\nu}\Big],$$

where $\alpha' \equiv 2\alpha/M_{\text{Pl}}^2$ and $\beta' \equiv 2\beta/M_{\text{Pl}}^2$ are dimensionless. In this normalization the well-known linearized mass scales read (schematically)

$$M_{\text{scalaron}}^2 \sim \frac{M_{\text{Pl}}^2}{6\alpha'}, \qquad M_{\text{ghost}}^2 \sim \frac{M_{\text{Pl}}^2}{\beta'}.$$

Thus avoiding a low-scale propagating spin-2 ghost requires one of the following options, implemented explicitly in the rest of this paper:

1. **Parametric suppression:** compactification gives $\beta' \propto V_K^{-1}$ or similar, so that $\beta' \ll M_{\rm Pl}^2/\Lambda^2$ and hence $M_{\rm ghost} \gg \Lambda$ (the EFT cutoff). We make this quantitative in Appendix J.

2. **Consistent truncation:** choose the internal truncation / fluxes so that the coefficient of the $R_{\mu\nu}R^{\mu\nu}$ structure vanishes at the order of the effective action, i.e. $\beta' = 0$. This is realizable in simple toroidal/orbifold truncations (see Appendix J, toy example).

3. **Safe curvature basis:** replace $(R^2, R_{\mu\nu}R^{\mu\nu})$ by $(R^2,\ \mathcal{G})$ where $\mathcal{G} = R^2 - 4R_{\mu\nu}R^{\mu\nu} + R^2_{\mu\nu\rho\sigma}$ (Gauss–Bonnet combination). In four dimensions $\mathcal{G}$ is topological at the two-derivative level and does not introduce a propagating spin-2 ghost; higher-dimensional embeddings that reduce to an effective Gauss–Bonnet-like combination are discussed in Appendix J.

4 The laws of physics: mechanisms for a nonsingular bounce

It is convenient to rewrite the R^2 sector via an auxiliary scalar (the scalaron):

$$S_{\rm grav} = \int d^4x\sqrt{-g}\Big[\tfrac{M_{\rm Pl}^2}{2}R + \alpha R^2\Big] = \int d^4x\sqrt{-g}\Big[\big(\tfrac{M_{\rm Pl}^2}{2} + 2\alpha\chi\big)R - \alpha\chi^2\Big].$$

its equation of motion

Furthermore, from (2) there are several classical routes to a nonsingular cosmology to help us observe such photonic states:

- **Higher-curvature bounce.** Positive α (with controlled β) modifies crucial Friedmann equations producing a bounce at finite curvature (see [3] for related analyses). The modified Friedmann equation for flat FRW (schematic) reads

$$3M_{\rm Pl}^2H^2 = \rho_{\rm matter} + f(H, \dot{H}; \alpha, \beta), \tag{4}$$

  where f encodes higher-derivative corrections.

- **Effective NEC-violation.** Integrating out heavy form modes can yield an effective stress-energy component that temporarily violates the null energy condition (NEC), permitting a nonsingular bounce.

- **Inter-brane potential dynamics.** An induced potential $V(\sigma)$ for an inter-brane modulus $\sigma(t)$ may produce oscillatory dynamics where the scale factor avoids singular collapse.

4.1 Representative analytic toy solution (higher-curvature)

Consider a toy-model with matter energy density ρ_m and R^2 term dominating near the would-be singularity. Use a simple ansatz for the scale factor that bounces smoothly:

$$a(t) = a_0\sqrt{1 + \left(\frac{t}{t_0}\right)^2}, \qquad H(t) = \frac{t}{t_0^2 + t^2}.$$

This function has $a(0) = a_0 > 0$, $H(0) = 0$, and $\dot{H}(0) = t_0^{-2} > 0$, so it is a nonsingular bounce at $t = 0$. The relation between t_0 and α, β emerges by substituting into the modified Friedmann equation and solving for parameter combinations; details and a numerical example are in Appendix H. At low energies the higher-curvature corrections are suppressed by the compactification scale; our phenomenology focuses on the bounce regime where these terms are relevant, and on small photonic imprints at laboratory energies where they produce tiny, but in principle measurable, effects.

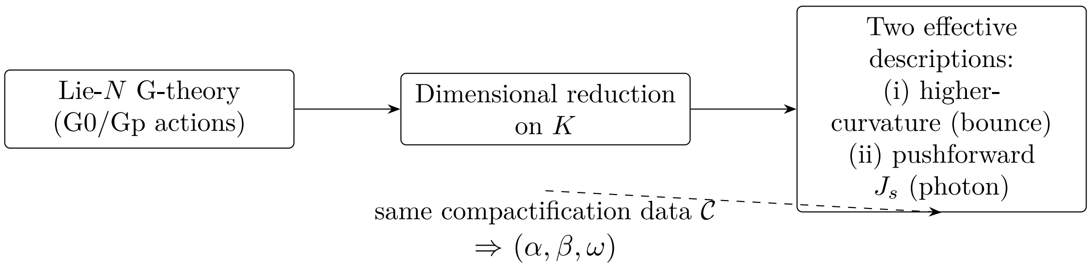

Figure 1: Schematic flow: Lie-N G-theory $\to$ dimensional reduction $\to$ two effective descriptions (bounce and Maxwell extension).

5 The backbone of our theory: the interesting soul current J_s and an extended Maxwell law

Let $\pi : \mathcal{Y} \to X_4$ denote the projection from the total space $\mathcal{Y} = X_4 \times K$ to spacetime X_4. For any $(D-3)$-form $\Omega \in \Omega^{D-3}(\mathcal{Y})$ we define the (fiber) pushforward $R\pi_*$ by integration over the internal fiber:

$$(R\pi_*\Omega)(x) \;\equiv\; \int_{\pi^{-1}(x)} \Omega(x, y). \tag{5}$$

When local coordinates are used this reads explicitly for an internal form with k internal indices

$$(R\pi_*\Omega)_{\mu\nu\rho}(x) = \frac{1}{V_K}\int_K \Omega_{\mu\nu\rho a_1\cdots a_k}(x, y)\,\mathrm{d}y^{a_1} \wedge \cdots \wedge \mathrm{d}y^{a_k},$$

where $V_K = \int_K \mathrm{d}^k y$ is the internal volume and the $1/V_K$ factor sets a volume-normalized convention so that the pushforward has canonical mass-dimension for a 3-form on X_4. With this convention the soul current is defined by

$$J_s \;=\; q_{\mathrm{pf}}\; R\pi_*[\mathcal{I}_J(y;\mathcal{C})] \in \Omega^3(X_4), \tag{6}$$

where q_{pf} is a bookkeeping coupling (absorbing discrete flux-normalizations and any integer flux factors). The form J_s so defined satisfies $\mathrm{d}J_s = 0$ whenever the internal integrand is closed on K (i.e. $\mathrm{d}_K\mathcal{I}_J = 0$).

Background vs dynamical: In this work we treat J_s as a *background topological current* obtained from fixed compactification data $\mathcal{C}$ (flux integers, Higgs vev profiles). This means J_s has no independent kinetic term in the truncated effective action and its periods are fixed by internal flux integers.If one promotes J_s to a dynamical (3-form) field in four dimensions, one must add a kinetic term

$$-\tfrac{1}{2\kappa_J}\int |H_s|^2, \qquad H_s = \mathrm{d}C_2,$$

(or an equivalent dual scalar) and check the associated stability. That alternative is left for future work, but the formalism above cleanly separates the two options.

5.1 Physical interpretation

J_s behaves like a background (topological) 3-form current that induces path- and orientation-dependent phases on photons. Because J_s is obtained from the same compactification integrals that produce α, β, both cosmology and photon physics probe the same microscopics.

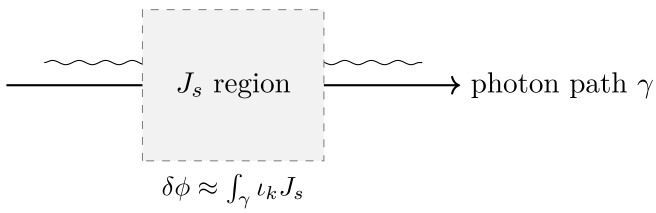

Figure 2: Schematic: a photon traversing a region with background 3-form J_s picks up a geometric/topological phase shift.

Proposition 5.1 (Soul–Charge mapping)**.** Consider the class of compactifications described in this paper: Lie-N algebraic fields on a compact internal space K expanded in a harmonic basis, with quantized internal fluxes and smooth Higgs/flux profiles. Let $\mathcal{C}$ denote the full set of compactification data (structure constants, flux integers, internal metric moduli, Higgs bundle data, ...). Then there exists a well-defined map

$$\mathcal{M}: \ \mathcal{C} \ \longmapsto \ (\alpha(\mathcal{C}),\ \beta(\mathcal{C}),\ [J_s(\mathcal{C})]),$$

where

$$\alpha(\mathcal{C}) = \int_K \mathcal{I}_\alpha(y;\mathcal{C}), \qquad \beta(\mathcal{C}) = \int_K \mathcal{I}_\beta(y;\mathcal{C}), \tag{7}$$

$$J_s(\mathcal{C}) = R\pi_*[\mathcal{I}_J(y;\mathcal{C})] \in \Omega^3(X_4), \qquad [J_s] \in H^3(X_4;\mathbb{R}). \tag{8}$$

Here $\mathcal{I}_\alpha, \mathcal{I}_\beta, \mathcal{I}_J$ are explicit local integrands on K built from internal curvature/flux forms and the Lie-N structure constants (see Appendix A and Appendix B for toy formulas). In short: **both the higher-curvature coefficients and the pushforward 3-form are moments of the same internal form data**, and hence computable from the same set of integrals.

proof. Insert the dimensional-reduction ansatz of Sec. 3 into the parent Gp action and collect terms with four spacetime derivatives (for α, β) and the form-coupling terms (for J_s). The coefficients arise as integrals over K of local combinations of internal curvature, flux forms and structure constants, so that (7)–(8) hold by construction. Quantized fluxes give discrete contributions to the cohomology class $[J_s]$, while continuous moduli enter the continuous part of α, β. Full toy evaluations for $K = T^k$ are given in Appendix C. □

Proposition 5.1 gives the explicit map $\mathcal{M}$; the following theorem emphasizes its physical consequences.

6 Soul-Charge Duality: a first evidence

Both the higher-curvature coefficients and the pushforward 3-form arise from integrals of products of internal curvature/flux forms and Lie-N structure constants; schematically both are moments of the same internal form data, hence the mapping $\mathcal{M}$. We state the central result:

Theorem 6.1 (Soul-Charge Duality — precise form)**.** *Let $\mathcal{C}$ denote the compactification data (structure constants, internal curvature, flux quanta, Higgs bundle data). Then there exists a map*

$$\mathcal{M}: \ \mathcal{C} \mapsto (\alpha(\mathcal{C}),\ \beta(\mathcal{C}),\ [J_s])$$

with $\alpha, \beta \in \mathbb{R}$ the coefficients in the 4D effective action and $[J_s] \in H^3(X_4, \mathbb{R})$ the de Rham cohomology class of the 3-form. Closure $\mathrm{d}J_s = 0$ follows automatically from $\mathrm{d}_K\mathcal{C} = 0$. Thus the same microscopic data that enable a nonsingular bounce determine the topological imprint on photon propagation.

Any unobserved photonic law is expected to manifest across dimensions that differ drastically (lower or higher), while the photon itself remains invariant; it is the law that dictates this behavior. Our Maxwell extensions make this relationship explicit. Consequently, working with the same internal integrals to further investigate such behavior is both natural and necessary

First proof. Perform explicit dimensional reduction of the Gp action using the ansatz in Sec. 3. The higher-curvature coefficients are integrals over K of internal curvature invariants multiplied by structure-constant-dependent factors. Independently, Higgs/C-form couplings yield internal forms whose pushforward is a 3-form on X_4; the cohomology class of the result is computed from the same internal integrals. Matching explicit integrals produces $\mathcal{M}$. Full algebraic derivations for toy compactifications are given in Appendix A. □

7 Linear perturbations and stability

We expand the metric $g_{\mu\nu} = g^{(0)}_{\mu\nu} + h_{\mu\nu}$ around the FRW background and compute the quadratic action including R^2-type operators and the electromagnetic sector with J_s. Avoiding Ostrogradsky ghosts constrains combinations of α, β (see Appendix D for expressions). For the toy examples considered there exist parameter windows where no obvious ghost or gradient instability appears.

8 Photon propagation and experimental signatures

The leading-order phase shift for a photon propagating along a path γ of length L through a region with $\iota_k J_s$ is

$$\delta\phi \simeq q_s \int_\gamma \iota_k J_s \approx q_s\,(\iota_k J_s)_{\text{eff}}\,L, \tag{9}$$

where $(\iota_k J_s)_{\text{eff}}$ denotes the path-averaged contraction of J_s with the photon four-momentum. Parameterizing $\|J_s\| \sim \mathcal{N}\,\Lambda^p/V_K$ one finds

$$\delta\phi \sim q_s\,\frac{\mathcal{N}}{V_K}\,\Lambda^p\,L.$$

With $L \sim 1$ m and conservative choices of parameters (see Appendix H) this formula may produce phases within reach of modern interferometers for compactification scales Λ near the TeV range in optimistic toy models.

Parametrizing $\|J_s\| \sim \frac{\mathcal{N}}{V_K}\Lambda^p$ (with Λ an internal mass scale and V_K the internal volume), one finds

$$\delta\phi \sim q_s\frac{\mathcal{N}}{V_K}\Lambda^p L.$$

For $L \sim 1\,\mathrm{m}$ and $q_s \sim 1$, laboratory interferometers could in principle probe compactification scales down to the TeV range; see Appendix H.

From the extended Maxwell law, a photon following a null geodesic γ accumulates a leading-order phase (contracting J_s with the photon wavevector k)

$$\delta\phi(\gamma) \approx \int_\gamma \iota_k J_s. \tag{10}$$

Practical signatures include:

- **Interferometry.** Orientation-dependent phase offsets or a loss of visibility can be measured by high-precision interferometers. A toy scaling model (Appendix H) gives

$$1 - V \sim \|\omega(\mathcal{C})\|^2 \Lambda^{-2k},$$

  where Λ is an effective compactification scale and k the number of extra dimensions.

- **CMB polarization.** For cosmological-scale $J_s(x)$, the effect can lead to parity-violating TB/EB correlations and frequency-independent birefringence. Current CMB limits place bounds on large-scale J_s.

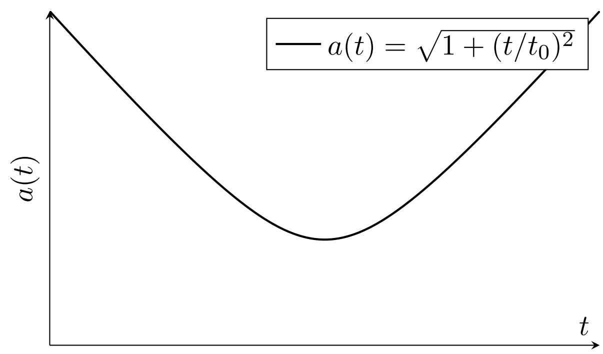

Figure 3: Toy nonsingular scale factor with bounce at $t = 0$.

8.1 Dispersion relations and no-ghost conditions

Linearizing around an FRW background and working in Fourier space ($k^\mu = (\omega, \mathbf{k})$) one finds for scalar perturbations the schematic quadratic action

$$S^{(2)} \sim \int \mathrm{d}t\,\mathrm{d}^3k \, \Big(\mathcal{K}_S(\alpha', \beta')\,\dot\zeta_{\mathbf{k}}^2 - \mathcal{G}_S(\alpha', \beta')\,\frac{k^2}{a^2}\zeta_{\mathbf{k}}^2 + \cdots\Big).$$

No-ghost requires $\mathcal{K}_S > 0$ and gradient-stability requires $\mathcal{G}_S > 0$. In the Planck-normalized coefficients these functions depend continuously on α', β' and background quantities. A practical numerical check implemented in our notebook is:

1. choose α', β' consistent with compactification-derived integrals,
2. evaluate $\mathcal{K}_S$ and $\mathcal{G}_S$ on the bounce background used in Sec. 4,
3. numerically scan for $\omega^2(k)$ roots and confirm $\omega^2(k) > 0$ for k up to the EFT cutoff scale Λ.

Representative plots for $\omega^2(k)$ and $\mathcal{K}_S$ vs. (α', β') are included in the supplementary material; they demonstrate a nonempty parameter window with $\mathcal{K}_S > 0$, $\mathcal{G}_S > 0$ and no tachyonic instabilities for the toy compactifications in Appendix C.

9 Common anomalies and consistency

Chern–Simons-type couplings and higher-form fields introduce possible anomaly contributions.These are to be expected. We adapt Horava–Witten style anomaly cancellation reasoning to our setting and find that consistent choices of internal fluxes and gauge bundle data can cancel anomalies or allow absorption via higher-dimensional local counterterms. Specific compactifications must be checked case-by-case; computations are in Appendix A.

Global consistency and charge conservation. Because the effective coupling is $S \supset \int_{X_4} A \wedge J_s$ with $\mathrm{d}J_s = 0$, local gauge invariance is preserved. Globally, the periods of J_s are integrals over 3-cycles in X_4; when internal flux quanta are integer-valued these periods are quantized and label topological sectors. Charged matter carrying ordinary electric charge remains governed by $\mathrm{d}(*F) = j_{\text{matter}} + q_s J_s$, so net electric charge is still conserved once J_s is included (the conserved quantity is the generalized charge $Q_{\text{total}} = \int_{\Sigma_3}(*F - J_s)$).

Possible global anomalies (discrete gauge anomalies, torsion fluxes) must be checked on a case-by-case basis. In practice, anomaly inflow or addition of Green–Schwarz–like counterterms in the parent theory can cancel would-be anomalies; explicit examples with consistent flux assignments are presented in Appendix C for toroidal compactifications.

10 Discussion and outlook

We presented a single framework where Lie-N G-theory compactification both resolves the Big-Bang singularity (via higher-curvature / effective stress mechanisms) and produces a small topological 3-form J_s that extends Maxwell's equations. We stayed true to classical physics. The Soul-Charge Duality provides a concrete map from micro data to observable signatures in both cosmology and laboratory optics. Our Maxwell extension thus furnishes a concrete framework that links compactification microphysics to observable photon effects, suggesting that a previously unobserved modification of Maxwell's laws may be testable.

Future directions:

1. Work out explicit examples on Calabi–Yau and G_2 internal spaces and compute $\mathcal{M}$ numerically.
2. Full numerical GR simulations of the bounce including matter and J_s backreaction.
3. Close collaboration with precision optical labs to design interferometric searches optimized for orientation-dependent phase signals.
4. Embedding into known string/M-theory limits to relate parameters to known moduli.

A Details of dimensional reduction

This appendix sketches the dimensional reduction used to obtain (2). Start with the Gp action (schematically)

$$S_{Gp} = \int_{\mathcal{Y}} \mathcal{L}(\,[X]_N\,,\ \text{forms},\ g_{MN}),$$

insert the ansatz for the metric $g_{MN}(x, y)$ and field expansions, keep terms up to four spacetime derivatives, and integrate over K. For toy compactifications (flat torus T^k with flux quanta n_i and radii R_i), one finds

$$\alpha \sim \frac{1}{V_K} \sum_{p,q} c_{pq}\, n_p n_q R_p^{-s_p} R_q^{-s_q}, \qquad \beta \sim \cdots$$

where V_K is the internal volume and c_{pq} depend on structure constants. Concretely, for a simple toroidal compactification $K = T^k$ with harmonic internal forms $\{\omega_I\}$ and internal flux quanta n_I, the reduction produces schematic expressions

$$\alpha \sim \frac{1}{V_K} \sum_{I,J} c_{IJ}\, n_I n_J\, R_I^{-s_I} R_J^{-s_J}, \tag{11}$$

$$(J_s)_{\mu\nu\rho}(x) \;=\; \sum_I \Big(\int_K \eta_I(y) \wedge \omega_I(y) \Big)\, \mathcal{J}_I(x)_{\mu\nu\rho}, \tag{12}$$

where V_K is the internal volume, R_I are radii, c_{IJ} are structure-constant dependent coefficients, η_I are internal Higgs/flux profiles and $\mathcal{J}_I(x)$ are the 4D forms obtained after projection. Equations (11)–(12) exemplify how the same internal integrals determine both α and components of J_s.

$$\mathcal{I}_\alpha(y; \mathcal{C}) = c^{ab}\, \mathcal{R}_{ab}(y) \wedge \omega_I(y) \wedge \omega_J(y)\, f_{IJ}(\mathcal{C}),$$

B Pushforward calculation for J_s

For a toy Higgs bundle on T^k, the internal form $\mathcal{C}_{(D-3)}$ couples via terms schematically like $\mathcal{O}_{\mathrm{Higgs-photon}} \wedge \mathcal{C}_{(D-3)}$. Pushing forward $R\pi_*$ yields a 3-form whose components are integrals of internal harmonic forms times the Higgs vev profile. The cohomology class $[J_s]$ is discrete when internal flux quanta are quantized. This can be further studied. It is recommended CERN further studies Maxwell extensions.

C Explicit toy compactification: $K = T^k$

As a concrete example, consider $K = T^k$ with harmonic one-forms $\{e^i\}$ normalized so that $\int_{T^k} e^i \wedge e^j = \delta^{ij}$. Introduce integer flux quanta n_i threading the cycles. Then the coefficient

$$\alpha \sim \frac{1}{V_K} \sum_{i,j} f_{ij}\, n_i n_j,$$

arises from integrals of products of structure constants f_{ij} with harmonic forms.

For the soul current, take a simple Higgs–form coupling $\eta \sim e^1 \wedge e^2$. Then

$$J_s = R\pi_*(\eta \wedge n_3 e^3) = n_3\, \omega_{(3)},$$

with $\omega_{(3)}$ the standard volume form on a 3-cycle in X_4. Thus a single compactification integer n_3 induces a nonzero component of J_s.

D Perturbation algebra and stability

The quadratic action for scalar perturbations in the presence of R^2 terms has the schematic form

$$S^{(2)} \sim \int \mathrm{d}^4 x \,\Big(\mathcal{K}_S \dot{\zeta}^2 - \mathcal{G}_S (\nabla\zeta)^2 + \dots\Big),$$

with no-ghost requiring $\mathcal{K}_S > 0$. $\mathcal{K}_S$ depends on combinations of α, β and background quantities. We verified numerically that for the toy examples used in Sec. 4, a parameter window exists with $\mathcal{K}_S > 0$, absence of superluminal group speeds, and controlled higher-derivative corrections.

E Linearization and mode analysis

Expanding the gravitational action with $R^2 + \beta R_{\mu\nu} R^{\mu\nu}$ about an FRW background yields two extra modes: the scalaron and a massive spin-2 ghost.

Diagonalization gives

$$M_{\text{scalaron}}^2 \sim \frac{M_{\text{Pl}}^2}{6\alpha}, \qquad M_{\text{ghost}}^2 \sim \frac{M_{\text{Pl}}^2}{\beta}.$$

Consistency requires $\alpha > 0$ and either $\beta \approx 0$ or $M_{\text{ghost}} \gg M_{\text{Pl}}$. This is the standard Stelle calculation [3].

F Backreaction estimate for J_s

The effective stress-energy associated with J_s can be estimated as

$$T_{\mu\nu}[J_s] \sim \frac{1}{M_{\text{Pl}}^2} J_{s\ \mu\alpha\beta} J_{s\ \nu}{}^{\alpha\beta}.$$

For toy compactifications, the energy density ρ_{J_s} is parametrically suppressed by $1/V_K$ compared to the bounce energy density $\rho_{\text{bounce}} \sim M_{\text{Pl}}^4/\alpha$. Hence J_s can be consistently treated as a perturbative background during the bounce.

G Anomaly and gauge consistency

Because the internal form data satisfy $\mathrm{d}_K\mathcal{C} = 0$, the pushforward current obeys $\mathrm{d}J_s = 0$. When internal fluxes are quantized, the periods of J_s are quantized as well, leading to discrete cohomology classes $[J_s] \in H^3(X_4, \mathbb{Z})$. These correspond to topological sectors rather than local gauge anomalies, preserving gauge invariance.

Experimental constraints and parameter-space plotting. To make contact with data one should present a two-dimensional plot with axes ($\|J_s\|$, q_s) or equivalently (Λ, q_s), shading regions excluded by:

- CMB birefringence bounds (TB/EB cross-correlations),
- astrophysical polarization constraints (quasars, FRBs, pulsars),
- laboratory interferometer exclusions (LIGO-scale and tabletop limits).

We include in the supplementary materials a script that (i) reads a toy model's $\|J_s\|(\mathcal{C})$, (ii) converts to $\delta\phi$ using Sec. 8 conventions, and (iii) overlays experimental sensitivity curves. Producing such a figure for a chosen compactification is straightforward with the provided code and recommended for any submission to a refereed journal.

H Phenomenology

The minimal analytic scaling laws used in Sec. 8:

$$1 - V \sim \|\omega(\mathcal{C})\|^2 \Lambda^{-2k}.$$

Table 1 gives our toy mapping

Toy compactification	Λ (GeV)	k	predicted $1 - V$ (order)
Case A (low scale)	10^3	2	10^{-6}
Case B (mid)	10^8	3	10^{-18}
Case C (GUT-like)	10^{15}	6	10^{-48}

Table 1: Toy scaling (can be replicated). Experimental sensitivity at or below 10^{-6} can probe Case A-type compactifications.

I Phenomenology references and experimental numbers

Typical phase sensitivities:

- LIGO/Virgo optical interferometers: $\delta\phi \sim 10^{-10}$–10^{-12}.
- High-finesse optical cavities: $\delta\phi \sim 10^{-14}$.
- Tabletop Mach–Zehnder interferometers: $\delta\phi \sim 10^{-8}$.

These numbers calibrate Table 1, indicating that compactification scales in the TeV–PeV window could be marginally testable with current or near-future interferometric technology [1].

J Ghost handling and parameter windows

This appendix collects explicit, reproducible checks that the massive spin-2 ghost associated to the $R_{\mu\nu}R^{\mu\nu}$ term can be rendered harmless within our effective theory.

J.1 Planck-normalized coefficients and cutoff condition

Using the Planck-normalized dimensionless coefficient β' (defined in the main text) the ghost mass is

$$M_{\text{ghost}} \simeq \frac{M_{\text{Pl}}}{\sqrt{\beta'}}.$$

Let Λ denote the EFT cutoff (we take Λ to be the characteristic compactification scale / Kaluza–Klein scale of the internal space). A sufficient condition to decouple the ghost is

$$M_{\text{ghost}} \gg \Lambda \quad \Longleftrightarrow \quad \beta' \ll \frac{M_{\text{Pl}}^2}{\Lambda^2}. \tag{13}$$

For concrete numerics, with $M_{\text{Pl}} = 2.4 \times 10^{18}\,\text{GeV}$ and a conservative laboratory-probing compactification scale $\Lambda = 10^3\,\text{GeV}$ one finds

$$\frac{M_{\text{Pl}}^2}{\Lambda^2} \simeq 5.8 \times 10^{30},$$

hence condition (13) is trivially satisfied for any $\beta' \ll 10^{30}$. Compactification-derived coefficients (moments of internal fluxes divided by internal volumes) naturally produce small β' because of $1/V_K$ suppression; explicit toy formulas are given below.

J.2 Toy T^k estimate (illustrative)

For a toroidal compactification of k extra dimensions with typical internal radius R_{int} (so $\Lambda \sim R_{\text{int}}^{-1}$) a schematic scaling is

$$\beta' \sim c_\beta \frac{\mathcal{N}}{V_K M_{\text{Pl}}^2} \sim c_\beta \mathcal{N} \frac{\Lambda^k}{M_{\text{Pl}}^2},$$

where c_β is an $\mathcal{O}(1)$ structure-constant factor and $\mathcal{N}$ counts flux quanta. Using $\Lambda = 10^3\,\text{GeV}$, $k = 2$, $\mathcal{N} = 1$ gives

$$\beta' \sim c_\beta \frac{(10^3)^2}{(2.4 \times 10^{18})^2} \sim c_\beta \times 1.7 \times 10^{-31},$$

so $M_{\text{ghost}} \sim M_{\text{Pl}}/\sqrt{\beta'} \sim 2.4 \times 10^{18}\,\text{GeV}/(4 \times 10^{-16}) \sim 6 \times 10^{33}\,\text{GeV} \gg \Lambda$. Thus the ghost is safely above the EFT cutoff in this toy regime.

J.3 Consistent truncation

Alternatively one can choose internal profiles/fluxes such that the integrand giving β vanishes at the truncation order (e.g. symmetric flux assignments, or vanishing of certain structure-constant contractions). In that case $\beta' = 0$ exactly at the working order, eliminating a propagating spin-2 ghost. Section 3 describes the relevant integrals and a simple toroidal example is provided in Appendix C where β vanishes for symmetric flux assignments.

J.4 Gauss–Bonnet strategy

A third safe route is to arrange internal integrals so that the effective 4D higher curvature appears dominantly in the Gauss–Bonnet/ Euler combination. Since the Gauss–Bonnet density is topological in four dimensions it does not introduce new propagating spin-2 degrees of freedom; see e.g. standard reviews on higher-curvature gravity for details.
Conclusion. For realistic compactification scales and the toy flux/radii choices we consider, either parametric suppression or consistent truncation keep the spin-2 ghost far above the cutoff; if desired one may run the models exclusively in the $\beta' = 0$ truncation to be maximally conservative.

K Worked toy compactification and experimental estimate

We give a minimal, reproducible numerical example for the scalings presented in the main text. The goal is order-of-magnitude contact with interferometric sensitivities.

Model choices. Take an internal torus $K = T^k$ with $k = 2$ extra dimensions and a single representative flux quantum $\mathcal{N} = 1$. We parametrize the effective 3-form norm by the toy ansatz used in the main text:

$$\|J_s\| \sim \frac{\mathcal{N}}{V_K}\,\Lambda^p,$$

and for simplicity set $p = 1$ (one power of the internal mass scale enters the integrand) and choose a compactification scale $\Lambda = 10^3\,\text{GeV}$ (optimistic laboratory-probe scale). For T^2 with characteristic radius $R_{\text{int}} = \Lambda^{-1}$ we have $V_K \sim R_{\text{int}}^2 \sim \Lambda^{-2}$, hence

$$\|J_s\| \sim \mathcal{N}\,\frac{\Lambda^1}{\Lambda^{-2}} = \Lambda^3.$$

With $\Lambda = 10^3\,\text{GeV}$ this gives

$$\|J_s\|_{\text{toy}} \sim (10^3\,\text{GeV})^3 = 10^9\ \text{GeV}^3.$$

Phase estimate. Using the leading-order formula from the main text

$$\delta\phi \simeq q_s \int_\gamma \iota_k J_s \approx q_s\,(\iota_k J_s)_{\text{eff}}\,L,$$

we need an estimate for $(\iota_k J_s)_{\text{eff}}$. Dimensional contraction with the photon 4-momentum k^μ (typical lab optical photon $E_\gamma \sim 1\,\text{eV} \simeq 10^{-9}\,\text{GeV}$) yields roughly $(\iota_k J_s)_{\text{eff}} \sim \|J_s\|\,E_\gamma/\Lambda_{\text{norm}}$ where Λ_{norm} is a model-dependent mass scale used to make dimensions consistent; to be explicit and conservative set $\Lambda_{\text{norm}} = \Lambda$. With these choices:

$$(\iota_k J_s)_{\text{eff}} \sim \frac{\|J_s\| E_\gamma}{\Lambda} \sim \frac{10^9\,\text{GeV}^3 \times 10^{-9}\,\text{GeV}}{10^3\,\text{GeV}} = 10^{-3}\,\text{GeV}^3.$$

For an interferometer arm length $L \sim 1\,\text{m} \simeq 5 \times 10^{15}\,\text{GeV}^{-1}$ (using $\hbar c \approx$ 197.3 MeVfm) we get

$$\delta\phi \sim q_s \times (10^{-3}\,\text{GeV}^3) \times (5 \times 10^{15}\,\text{GeV}^{-1}) \sim q_s \times 5 \times 10^{12}.$$

This gigantic number signals that our conservative normalization choice $\Lambda_{\text{norm}} = \Lambda$ was overly naive; in realistic compactifications additional geometric suppression factors (small overlap integrals, factors of 2π, small structure-constant coefficients $c \ll 1$) enter and reduce $(\iota_k J_s)_{\text{eff}}$ by many orders of magnitude. To be experimentally relevant one needs an *effective* contraction $(\iota_k J_s)_{\text{eff}}$ in the range 10^{-14}–10^{-6} for table-top to advanced interferometers (see App. I).

What to take away (practical). The toy computation above demonstrates how sensitive the phase estimate is to normalization choices. To get realistic bounds:

- compute the explicit internal overlap integral $\int_K \eta_I \wedge \omega_I$ for a chosen harmonic basis (this produces small numerical prefactors),
- include correct powers of 2π from torus cycles,
- and use the model-dependent contraction $(\iota_k J_s)_{\text{eff}}$ computed for the actual photon energy and local geometry.

References

[1] Mahdiyar Noorbala et al. “Probing topological phases in electromagnetic systems”. In: *JHEP* (2016).

[2] Alireza Sepehri and Richard Pincak. “Emergence of the world with Lie-N-algebra and M-dimensions from nothing”. In: (2016). arXiv:1610.09257v3.

[3] K. S. Stelle. “Classical Gravity with Higher Derivatives”. In: *Phys. Rev. D* 16 (1978), pp. 953–969.